UCRL-94277
PREPRINT

A 2D Lagrange MHD Code

R. E. Tipton

This paper was prepared for submittal to
Megagauss IIII Conference
Santa Fe, New Mexico
July 14–17, 1986

July 1986

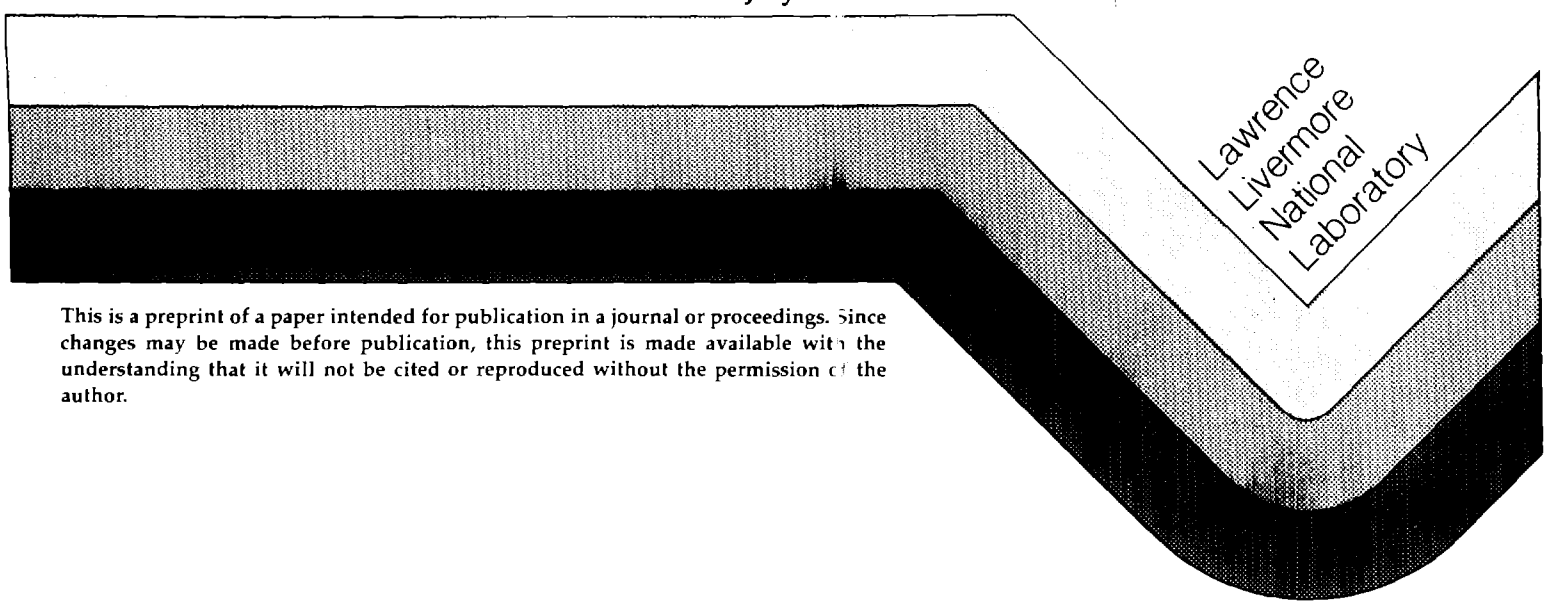

A 2D LAGRANGE MHD CODE*

R. E. Tipton

Lawrence Livermore National Laboratory
University of California
Livermore, California 94550

ABSTRACT

An MHD model has been implemented on a 2D Lagrangian mesh with cylindrical symmetry. The magnetic diffusion equations for both B_θ and B_r, B_z are solved. The code has been used to model several simple experiments involving induced currents in conducting rings. The calculated results have been compared with the experimental data. The goal of this research is to develop a detailed computational model to aid in the design of High Explosive Generators.

INTRODUCTION

In order to facilitate the design and study of magnetic flux compression generators, a two dimensional Magneto Hydrodynamic computer model is being developed. This paper briefly describes the hydrodynamic and magnetic equations which are solved, and presents the results of three test problems.

A Lagrangian formalism was selected rather than an Eulerian formalism in order to properly resolve thin metal parts, usually found in generators, without using an excessive total number of computational zones. In the future, an ALE (Arbitrary Lagrangian Eulerian) capability will be added, which will allow excessive distortions in the mesh to be smoothed out without any significant loss of accuracy. Equation of state and strength of material properties are modeled by a theoretical and empirical data base that has been adjusted to match a wide variety of independent experiments, for a large number of materials of interest.

The present code can solve for either B_θ or B_r, B_z as it also solves the hydrodynamic equations. The magnetic fields may be driven by source currents, or interact with an external circuit. In future versions of the code, B_θ, B_r, and B_z will be coupled together and solved simultaneously so that helical generators may be studied.

HYDRODYNAMICS

Conservation of Momentum

$$\rho \dot{\mathbf{U}} = \nabla \cdot \mathbf{S} + \mathbf{f}_Q + \mathbf{j} \times \mathbf{B}$$

ρ = Density

* Work performed under the auspices of the U.S. Department of Energy by the Lawrence Livermore National Laboratory under Contract W-7405-Eng 48.

U = Velocity

$$\mathbf{S} = -p\begin{bmatrix}1 & 0 & 0\\ 0 & 1 & 0\\ 0 & 0 & 1\end{bmatrix} + \begin{bmatrix}TRR & TRZ & 0\\ TRZ & TZZ & 0\\ 0 & 0 & T\theta\theta\end{bmatrix}$$ — Total Stress Tensor

P = Isotropic Pressure

$\mathbf{T}$ = Deviatoric Stress Tensor

$\mathbf{f}_Q$ = Forces Due to Artificial Viscosities

$\mathbf{j}$ = Current Density

$\mathbf{B}$ = Magnetic Field

Conservation of Energy

$$\dot{\epsilon} = -p\dot{V} + \dot{\epsilon}_Q + \frac{1}{\rho}\mathrm{Tr}(\dot{\mathbf{e}} \cdot \mathbf{T}) + \frac{c}{\rho}\mathbf{j} \cdot \mathbf{E}$$

ϵ = Specific Internal Energy

V = Specific Volume

$\dot{\epsilon}_Q$ = Heating Rate Due to Artificial Viscosities

$$\dot{\epsilon} = \begin{bmatrix} \frac{\partial \dot{r}}{\partial r} & \frac{1}{2}\left(\frac{\partial \dot{r}}{\partial z} + \frac{\partial \dot{r}}{\partial r}\right) & 0\\ \frac{1}{2}\left(\frac{\partial \dot{r}}{\partial z} + \frac{\partial \dot{z}}{\partial r}\right) & \frac{\partial \dot{z}}{\partial z} & 0\\ 0 & 0 & \frac{\dot{r}}{r}\end{bmatrix} - \frac{1}{3}\frac{\dot{V}}{V}\begin{bmatrix}1 & 0 & 0\\ 0 & 1 & 0\\ 0 & 0 & 1\end{bmatrix}$$

Deviatoric Strain Rate Tensor

c = Speed of Light

$\mathbf{E}$ = Electric Field

Conservation of Mass

$\dot{M} = 0$

M = Lagrangian Zonal Mass

In the Lagrange formalism, the mass moves with the mesh so it remains constant. From the updated coordinates, new zonal volumes are calculated and the new densities are found.

Equation of State

For many materials a Grüneisen equation of state with a cubic fit to the shock velocity particle velocity Hugoniot relation is used. Other materials use polynomial fits to theoretically or experimentally derived Hugoniots and adiabats.

Constitutive Model

For materials with strength, the Steinberg-Guinan constitutive model is used,[1] along with the Steinberg-Sharp strain rate dependence model.[2]

Finite Difference Scheme

Except for the artificial viscosities, the HEMP differencing scheme on an arbitrary quadrilateral mesh[3] is used to integrate the hydrodynamic equations. John White's artificial viscosity[4] is used combined with William Schulz's method of centering the artificial viscosity on a two dimensional quadrilateral mesh.[5]

MAGNETIC DIFFUSION

B_r, B_z Field

$$\frac{4\pi\sigma}{2\pi rc}\dot{\Phi} = \nabla \times \nabla \times A_\theta + 4\pi j_\theta + \frac{4\pi\sigma}{2\pi r}\Delta V$$

$\Phi = 2\pi r A_\theta$ — Magnetic Flux

A_θ = Vector Potential

σ = Electrical Conductivity

c = Speed of Light

j_θ = Source Current Density

ΔV = Voltage Drop Across External Circuit

$$B_r = -\frac{1}{2\pi r}\frac{\partial\Phi}{\partial z}$$ — r component of Magnetic Field

$$B_z = \frac{1}{2\pi r}\frac{\partial\Phi}{\partial r}$$ — z component of Magnetic Field

B_θ Field

$$\frac{4\pi}{c}\phi = \int_\Sigma ds\, \nabla \times \frac{1}{\sigma}\nabla \times B_\theta + 4\pi\Delta V$$

$$\varphi = \int_\Sigma ds\, B_\theta$$ — Magnetic Flux Inside Surface Σ

B = θ component of Magnetic Field

$$j_r = -\frac{1}{4\pi}\frac{\partial B_\theta}{\partial Z}$$ — r Component of Current Density

$$j_z = \frac{1}{4\pi r}\frac{\partial(rB_\theta)}{\partial r}$$ — z Component of Current Density

Units

C.G.S. E.M.U. Gaussian units are used. In this system of units, electric charge is measured in EMU's (Electro-Magnetic Units) which equals ESU (Electro-Static Unit) divided by the speed of light. The EMU is a more convenient unit than the ESU because the unit of electric current is EMU/sec which equals 1/10 amp. In order to preserve Ohm's law: $J = \sigma E$ where J has units of EMU/sec/cm^2 and E has units of ESU/cm^2, it is necessary for the electrical conductivity to be measured in the non-standard units of σ(ESU)/c. The standard ESU unit for conductivity is sec^{-1}, hence this non-standard unit becomes cm^{-1}. The magnetic field is still measured in Gauss.

Lagrange Time Derivative

The $\dot{\Phi}$ and $\dot{\varphi}$ appearing in the magnetic diffusion equations represent Lagrange time derivatives.

$$\dot{\Phi} = \frac{\partial \Phi}{\partial t} + \mathbf{U} \cdot \nabla \Phi \qquad \dot{\varphi} = \frac{\partial \varphi}{\partial t} + \mathbf{U} \cdot \nabla \varphi$$

$\dot{\Phi}$ and $\dot{\varphi}$ are the time derivatives as seen by a frame of reference locally at rest with fluid. The magnetic diffusion equations are written as time derivatives of Φ and φ rather than A_θ or B_θ because it is the extra factor of radius or area inside of the Lagrange time derivative which exactly accounts for the fact that the fluid is moving and a generalized form of Ohm's law should be satisfied:

$$\mathbf{j} = \sigma\left(\mathbf{E} + \frac{\mathbf{V}}{c} \times \mathbf{B}\right)$$

Conductivity Model

In the present code only a very simple model for the electrical conductivity is used:

$$\sigma = 1/(\eta_o + \eta_1 \Delta T)$$

This allows the electrical resistivity to vary linearly with temperature. Future versions of the code will include more complex and realistic conductivity models.

Finite Difference Scheme

It is impractical to difference the magnetic diffusion equations explicitly because the stability time step drops to zero in vacuum zones where the conductivity is near zero. It is therefore necessary to solve the equations implicitly. To do this, the $\nabla \times \nabla$ operator is represented as a symmetric banded matrix coupling Φ or φ in each zone to all eight of its nearest neighbors. This coupling matrix is then inverted by David Kershaw's ICCG method.[6] The coupling between two neighboring zones is determined by first constructing a dual mesh consisting of all the zone centers. Φ and φ are thought to "sit" at these points. The dual mesh will also contain arbitrary quadrilaterals. Each quadrilateral is divided into two sub-triangles. Alan Winslow's finite element method for determining the $\nabla \times \nabla$ coupling on a triangular mesh[7] is used with N. J. Diseren's modification.[8] Since there are two distinct ways of splitting a quadrilateral into two sub-triangles, each quadrilateral is split both ways and the resulting coupling matrices are averaged.

PROBLEM #1 SOLENOID ON AN IRREGULAR MESH

In order to test the accuracy of the differencing scheme for the $\nabla \times \nabla$ operator, an infinite solenoid problem was set up using an irregular mesh. A Θ source current was specified between the cylindrical radii of 1.0 cm and 1.1 cm such that the magnetic field should be 1.0 Gauss inside the solenoid and 0 outside. Magnetic reflection boundaries were specified at Z = 0 cm and Z = 10.0 cm. Hydrodynamics has been turned off. Since the exact solution to this problem is known, it provides a good test for the accuracy of the spatial differencing scheme used on an arbitrary quadrilateral mesh for solving the magnetic diffusion equations.

Figure 1a shows the irregular mesh. This mesh is much more distorted than many actual problems of interest. When the ALE automatic rezoning is added, even moderately turbulent problems should run without serious mesh distortion. The iso-contours of the magnetic flux Φ, is shown in Figure 1b. Note that the contours are straight and parallel to the axis showing no imprint of the irregular mesh. Figure 1c shows 1D slice plots of Φ vs. r for three places in the mesh. Deviations from the exact solution are too small to be visible in the plot. Figure 1d shows 1D slice plots of the magnetic field B_z vs. r for the same three places in the mesh. At the edges of the mesh, B_z is very close to the exact solution. In the middle of the mesh, however, where the mesh is more distorted, B_z differs from the exact solution by as much as 2%.

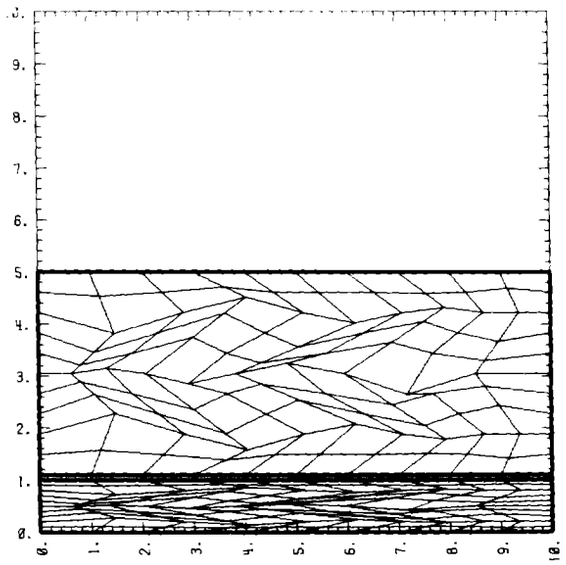

Fig. 1a. Irregular mesh used on problem #1.

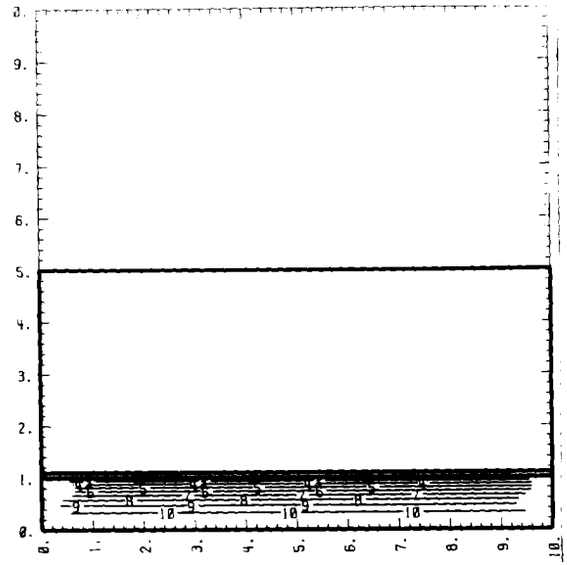

Fig. 1b. Iso-contour plot of the magnetic flux on problem #1. Contours are parallel to the axis, showing no imprint of the mesh.

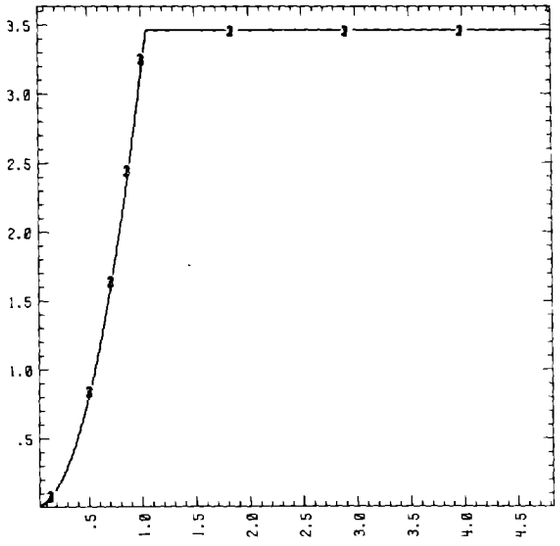

Fig. 1c. Magnetic flux versus radius for problem #1. The flux is within 1% of the exact solution.

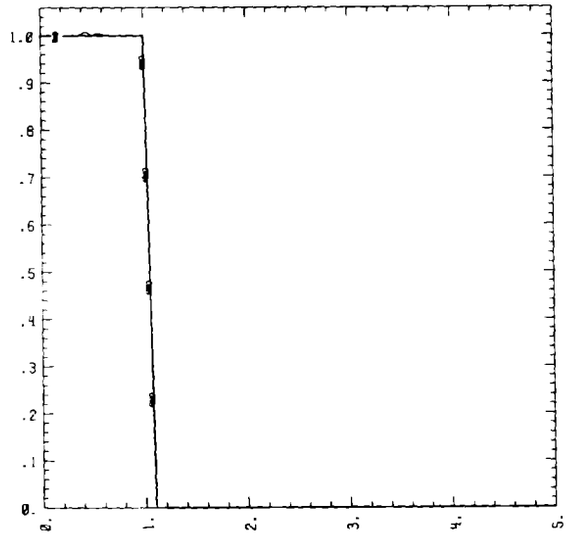

Fig. 1d. Magnetic field versus radius for problem #1. The field is within 2% of the exact solution.

PROBLEM #2 EXPANDING COPPER RING

Problem #2 is a calculation of an actual experiment. The experimental setup consists of a solenoid made out of six turns. Each turn was carefully wound to maintain axial symmetry. It was not wound as a helix. Around the mid-plane of this solenoid a copper ring was placed. A capacitor is discharged into the solenoid, driving a large current with a peak value of 23 kiloamps. The resulting current in the copper ring interacts with the magnetic field to cause a rapid radial expansion of the ring. The response current in the ring was diagnosed with a Rogowski coil. The velocity of the ring was measured with a Fabre-Perot Velocimeter.

Only half the problem needs to be included in the calculation because of symmetry. Figure 2a shows the three solenoid turns and the copper ring at 20 μsec, the time of peak ring velocity. Figure 2b

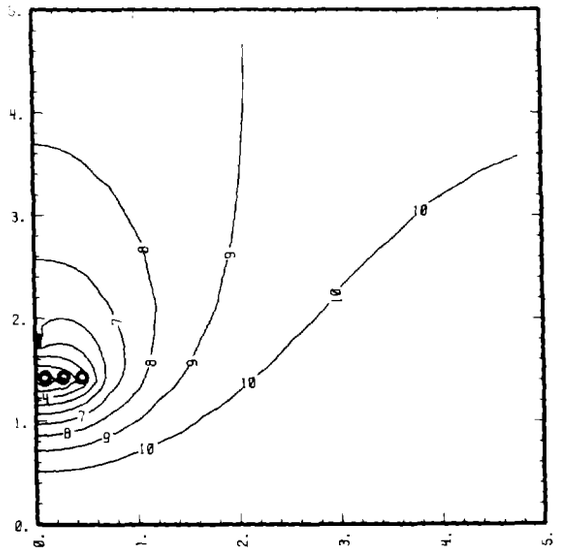

Fig. 2a. Global view of problem #2. Symmetry plane is on the left. Three solenoid turns and half the Cu ring are shown along with lines of mag. flux.

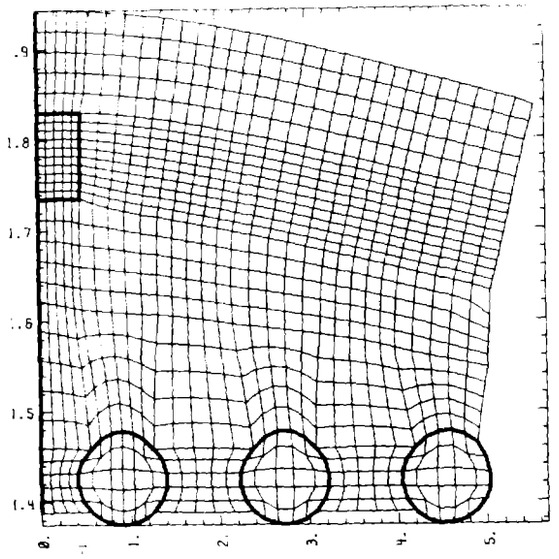

Fig. 2b. Blowup showing the computational mesh used in the solenoid/ring area. The ring has moved 0.18 cm by this time.

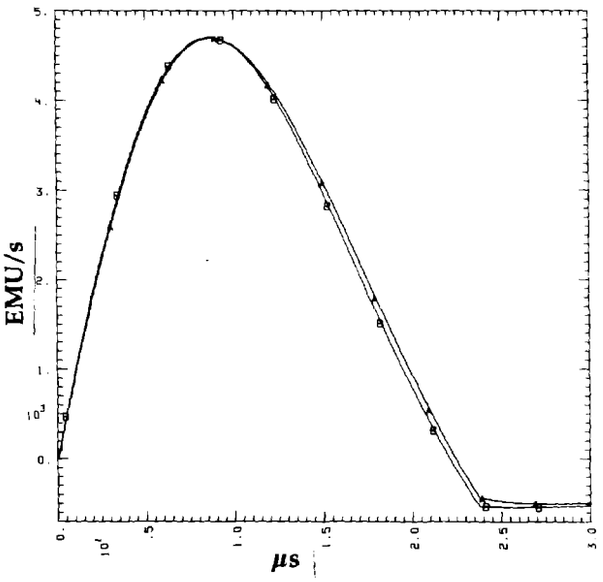

Fig. 2c. Comparison between the measured (Curve A) and calculated (Curve B) response current in the Cu ring.

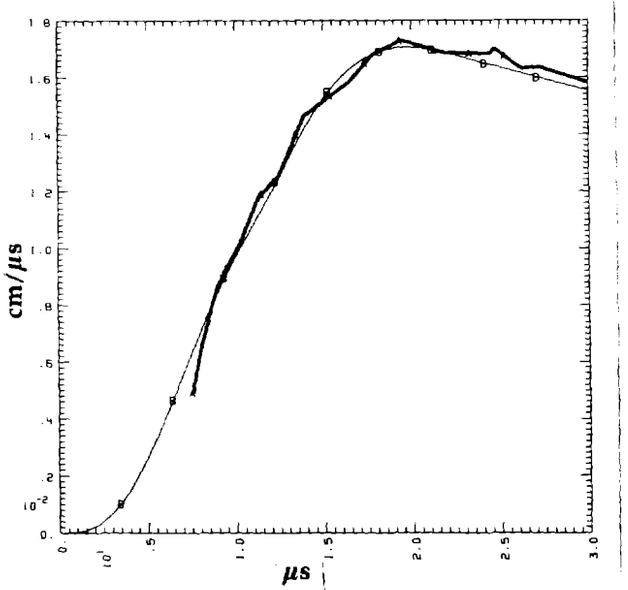

Fig. 2d. Comparison between the measured (Curve A) and calculated (Curve B) velocity of the Cu ring.

shows a blowup of the solenoid and ring area. Figure 2c shows the comparison between the measured and calculated response current in the copper ring. Note that the overall agreement is rather good. The agreement is very good up until the time of peak current. Figure 2d shows the comparison between the measured and calculated velocities of the copper ring. Note that within the scatter in the data, the agreement is good. The velocity in the calculation is more sensitive to the details of the strength model used rather than the MHD model.

PROBLEM #3 COAXIAL GENERATOR

Problem #3 is a calculation of a simple coaxial generator intended to illustrate the code's capability to solve problems with B_θ fields coupled to hydrodynamic motion and an external circuit. The problem

consists of a cylinder of PBX-9404, 8.8 cm in length and 2.0 cm in radius. Surrounding the explosive is a 1 mm thick cylindrical shell of copper. This inner copper shell is surrounded by a void, followed by an outer copper shell with an inner radius of 3.0 cm and an outer radius of 3.1 cm. At time zero, the explosive is detonated at z = 0 cm with a plane detonation pattern. At the same time, an external capacitor discharges into the generator. At 3 μsec, the capacitor has reached its peak current of 10^4 EMU/sec (10^5 amps) and the void in the generator is filled with a magnetic field of about 5 kilogauss. At this time the capacitor is switched out of the external circuit and the load is switched in. The inner copper shell continues to compress the magnetic field in the void until 12 μsec when a peak current of 1.6×10^6 EMU/sec (1.6×10^7 amps) is reached.

In order to perform this calculation, it was necessary to add a void closure routine to the code. This routine simply converts void zones into copper zones whenever the volume of the void zone reaches a

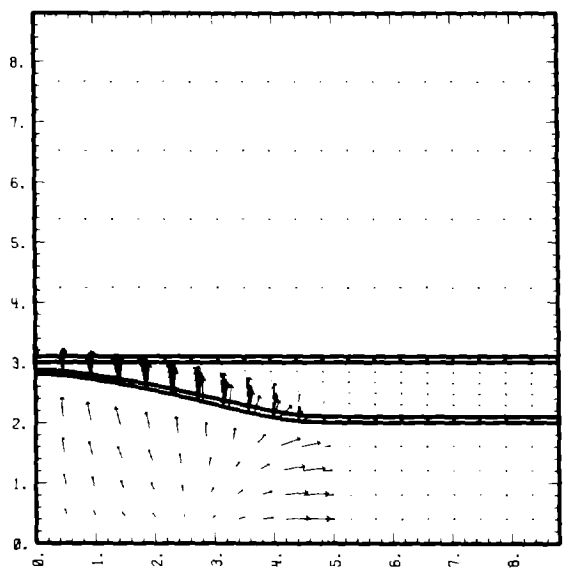

Fig. 3a. Coaxial generator at 5 μs. Half the explosive has detonated. The void contains a magnetic field of 5 kilogauss.

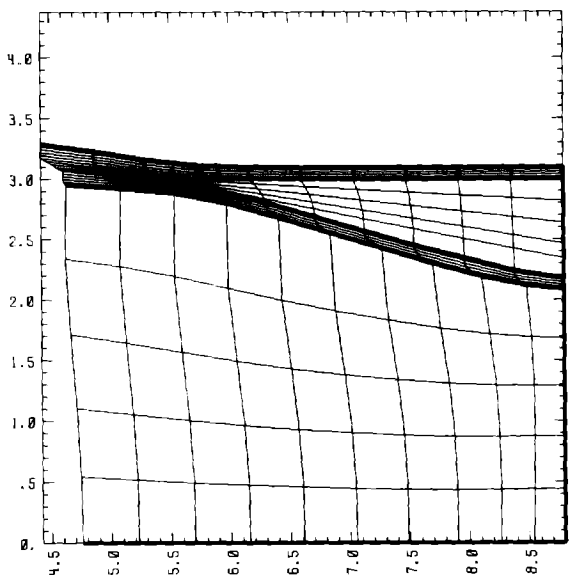

Fig. 3b. Blowup of contact region at 10 μs showing that void zones are converted to Cu.

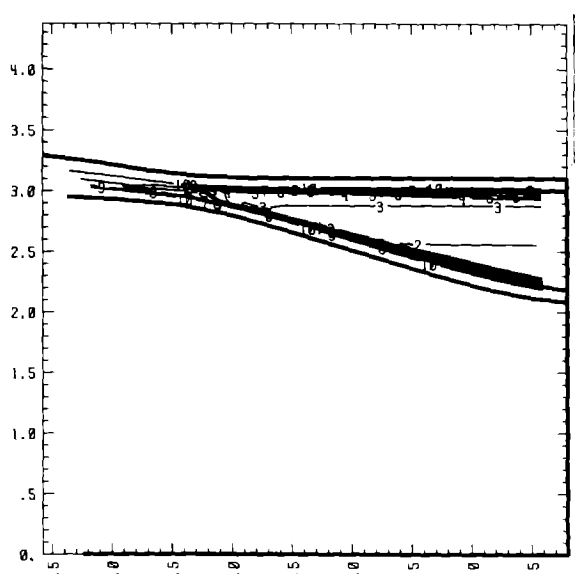

Fig. 3c. Contact region at 10 μs showing lines of constant B_θ. Most of the magnetic field is in the void with strong gradients at Cu surfaces. Some magnetic field is trapped behind contact point.

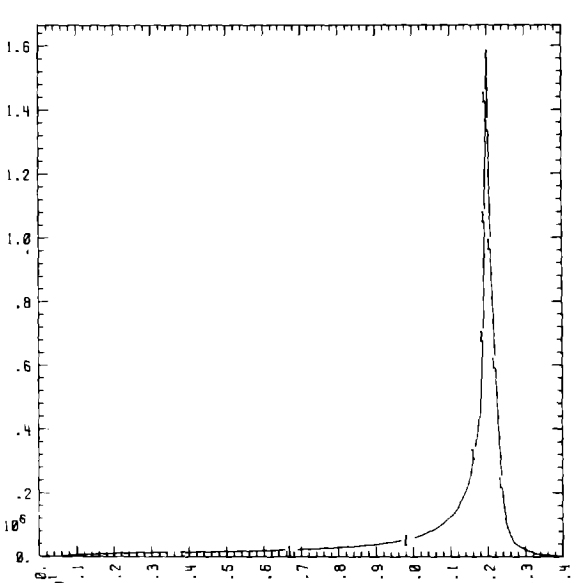

Fig. 3d. Output current of generator in EMU/s. The initial current of 10^4 EMU/s (10^5 amps) has been amplified by 160.

reasonably small value. This conversion is done in such a way that momentum, energy and magnetic flux are conserved.

Figure 3a shows the generator 5 μsec after the detonation begun. This is just before the two copper cylinders make contact. Figures 3b, 3c and 3d show blowups of the contact region at 10 μsec, showing, among other things, that some of the magnetic flux becomes trapped behind the contact point and cannot contribute to the output of the generator.

REFERENCES

1. D. J. Steinberg, S. G. Cochran, and M. W. Guinan, A constitutive model for metals applicable at high-strain rate, J. Appl. Phys., 51(3):1498 (1980).

2. D. J. Steinberg and R. W. Sharp, Jr., J. Interpretation of shock-wave data for beryllium and uranium with an elastic-visco plastic constitutive model, J. Appl. Phys., 52(8):5072 (1981).

3. M. L. Wilkins, Calculation of elastic-plastic flow, in "Methods of Computational Physics," B. J. Alder, S. Fernbach, and M. Rotenberg, eds., Academic Press, New York (1964), vol. III.

4. John White, A new form of artificial viscosity:postscript, J. Comp. Phys., 12:553 (1973).

5. W. D. Schulz, Two-dimensional Lagrangian hydrodynamic difference equations, in: "Methods of Computational Physics," B. J. Alder, S. Fernbach, and M. Rotenberg, eds., Academic Press, New York (1964), vol. III.

6. D. S. Kershaw, The incomplete Cholesky-conjugate gradient method for the iterative solution of systems of linear equations, J. Comp. Phys., 26:43 (1978).

7. A. M. Winslow, Numerical solution of the quasilinear Poisson equation in a non-uniform triangle mesh, J. Comp. Phys., 1(2):149 (1967).

8. N. J. Diserens, "Further Development of the Magnetostatic Computer Programm TRIM at the Rutherford Laboratory," Rutherford High Energy Laboratory, Chilton Didcot Berkshire, England, RHEL/R (1969).